Applied Physics B (2018) 124:8
https://doi.org/10.1007/s00340-017-6878-5

Applied Physics B
Lasers and Optics

Detection of carbon monoxide (CO) in sooting hydrocarbon flames using femtosecond two-photon laser-induced fluorescence (fs-TPLIF)

Yejun Wang[1] · **Waruna D. Kulatilaka**[1]

Received: 23 August 2017 / Accepted: 6 December 2017 / Published online: 18 December 2017

Abstract
Ultrashort-pulse, femtosecond (fs)-duration, two-photon laser-induced fluorescence (fs-TPLIF) measurements of carbon monoxide (CO) are reported in rich, sooting hydrocarbon flames. CO-TPLIF detection using conventional nanosecond or picosecond lasers are often plagued by photochemical interferences, specifically under fuel-rich flames conditions. In the current study, we investigate the commonly used CO two-photon excitation scheme of the $B^1\Sigma^+ \leftarrow X^1\Sigma^+$ electronic transition, using approximately 100-fs-duration excitation pulses. Fluorescence emission was observed in the Ångström band originating from directly populated $B^1\Sigma^+$ upper state, as well as, in the third positive band from collisionally populated $b^3\Sigma^+$ upper state. The current work was focused on the Ångström band emission. Interference from nascent C_2 emissions originating from hot soot particles in the flame could be reduced to a negligible level using a narrower detection gate width. In contrast, avoiding interferences from laser-generated C_2 Swan-band emissions required specific narrowband spectral filtering in sooting flame conditions. The observed less than quadratic laser pulse energy dependence of the TPLIF signal suggests the presence of strong three-photon ionization and stimulated emission processes. In a range of CH_4/air and C_2H_4/air premixed flames investigated, the measured CO fluorescence signals agree well with the calculated equilibrium CO number densities. Reduced-interference CO-TPLIF imaging in premixed $C_2H_4/O_2/N_2$ jet flames is also reported.

1 Introduction

Carbon monoxide (CO) is a major byproduct of incomplete oxidation during combustion of hydrocarbon fuels. In general, CO levels would increase under low-temperature, fuel-rich conditions and are regulated because of its toxic and harmful effects on the environment and human health. Moreover, emission of CO results in reduced combustion efficiency because of the main heat release reaction, $CO + OH \rightarrow CO_2 + H$ during complete oxidation of hydrocarbon fuels [1]. A detailed understanding of spatially and temporally resolved CO formation is, therefore, of significant importance in many practical combustion systems. Among several diagnostic approaches for in-situ detection of CO, laser-induced fluorescence (LIF) is the most promising technique because of its high sensitivity and ease of extension into 2D imaging [2]. However, the readily accessible lower electronic transitions of CO fall in the vacuum-ultraviolet (VUV) wavelength region where the medium becomes optically thick under most practical combustion conditions. Therefore, multi-photon excitation schemes such as two-photon laser-induced fluorescence (TPLIF) are often used to red shift the excitation wavelength to the ultraviolet (UV) region.

For TPLIF measurement of CO in combustion environments, several excitation/detection schemes have been investigated: (1) excitation of $C^1\Sigma^+ \leftarrow X^1\Sigma^+$ transition at 217-nm followed by detection of the $C^1\Sigma^+ \rightarrow A^1\prod$ Herzberg band emission in the 360–600 nm region, (2) excitation of $B^1\Sigma^+ \leftarrow X^1\Sigma^+$ transition at 230.1-nm radiation followed by detection of the $B^1\Sigma^+ \rightarrow A^1\prod$ Ångström band emission in the 400–600 nm region, and (3) same excitation scheme as in 2) but detection of the $b^3\Sigma^+ \rightarrow a^3\prod$ third positive band in the 282–380 nm wavelength region following vibrational redistribution [3, 4]. Most previously published studies of TPLIF detection of CO have used the 230.1-nm excitation and analysis of the fluorescence signals from the Ångström band [5–10].

Number of important parameters for quantitative CO measurements have also been the subject of numerous previous studies, for example, interferences due to photodissociation of CO_2 [1], collisional quenching [11, 12],

✉ Waruna D. Kulatilaka
waruna.kulatilaka@tamu.edu

[1] Department of Mechanical Engineering, Texas A&M University, College Station, TX 77843-3123, USA

photoionization [13, 14], stimulated emission [15], fluorescence lifetime [16], excitation cross section [11, 13], and collisional line broadening [17]. Another major interference when using the 230.1-nm excitation scheme in rich hydrocarbon flames is the crosstalk between strong C_2 Swan-band emissions in the overlapping spectral range of approximately 430–700 nm [18]. C_2 Swan-band emissions can significantly reduce the accuracy of measured CO concentrations. In addition, significant C_2 emissions can also be generated via photodissociation of hydrocarbon fuels or soot particles from the excitation laser itself [19–22]. The natural fluorescence lifetime of the CO $B^1\Sigma^+$ state is approximately 22 ns; however, collisional quenching at modest pressures significantly reduces the effective lifetime down to a few nanoseconds under practical combustion conditions [12]. Previous CO emission lifetime measurements have been reported using nanosecond (ns) [23, 24], as well as picosecond (ps) [12] pulsed lasers.

In a more recent study, Brackmann et al. [19] applied ps pulses to measure CO in premixed laminar flames. They also directly compared the ps results with ns excitation scheme. They concluded that ps pulses show stronger signal strengths, as well as reduction of C_2 interference, when a narrower detection gate width is employed. More recently, TPLIF detection studies of atomic species such as H, O and N, have also suggested that nearly Fourier-transform-limited, femtosecond (fs)-duration laser pulses can exhibit photolytic interference-free fluorescence measurements in flame and plasma systems [25–29]. The low-average power but high-peak-power fs pulses can enhance two-photon excitation efficiency and mitigate interferences from single-photon-absorption photodissociation processes. Therefore, the fs-TPLIF scheme has demonstrated the potential of interference-free 2D imaging measurements of important atomic species [27, 29]. This concept has also been extended recently for CO TPLIF detection using fs pulses [30].

In the present study, we apply fs-TPLIF to measure CO concentrations in rich sooting hydrocarbon flames. As indicated above, understanding CO formation becomes especially important in rich flames conditions, where significant levels of soot are also present. Therefore, we investigate possible interferences in a range of methane (CH_4) and ethylene (C_2H_4) sooting flames. Such studies are a first step towards understanding partial oxidation and soot formation chemistry in cold pockets and non-well-mixed regions of practice turbulent flames encountered in gas turbines and IC engines. The excitation/detection scheme along with the experimental details are presented in the next section. The subsequent "Results and discussion" section presents the details of CH_4 and C_2H_4 flame measurements along with two-dimensional (2D) imaging studies in stable premixed laminar flames at the end. A summary and a discussion along the future perspectives of fs-TPLIF imaging of CO are presented in the "Conclusions" section.

2 Experimental

As shown in Fig. 1, approximately 100-fs duration laser pulses centered at 230.1 nm excite the CO molecules from ground state ($X^1\Sigma^+$) to excited state ($B^1\Sigma^+$), then the fluorescence from the $B^1\Sigma^+ \rightarrow A^1\prod$ Ångström band in the range of 400–600 nm is detected. Furthermore, some CO molecules at $B^1\Sigma^+$ state relax to $b^3\Sigma^+$ state as a result of collisional energy transfer processes in the combustion system, thus fluorescence signal can also be detected from the $b^3\Sigma^+ \rightarrow a^3\prod$ third positive band in the 280–380 nm range. It can be seen that excitation at 230.1 nm and detection in the third positive system could eliminate most of C_2 and CH interferences in the 400–600 nm region. However, the third positive system exhibits strong pressure and collisional quenching dependencies as compared to the Ångström band [3], as well as, fluorescence occurs in the UV spectral region where detection cameras are less sensitive. Therefore, in the current experiments, we focus on the Ångström band emission to detect CO, while accounting for various interferences in sooting flames. Comparison of previously employed ns- and ps-duration pulses for TPLIF, as described above, shows that the fs-duration excitation scheme has advantages of strong signal generation and less susceptibility to interfering photodissociation processes. Therefore, this work is focused on investigating the potential of fs-TPLIF scheme in detecting CO in sooting flames while effectively suppressing C_2 photochemical interference.

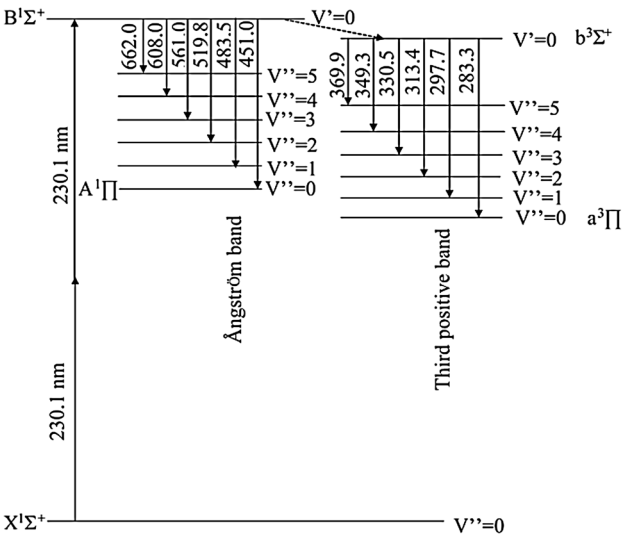

Fig. 1 Energy-level diagram of femtosecond two-photon LIF of CO

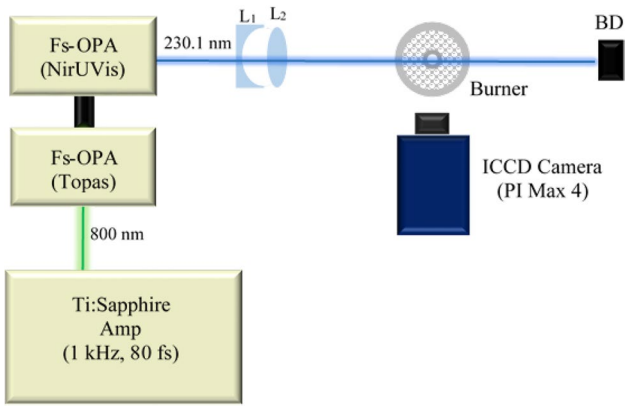

Fig. 2 Schematic diagram of the experimental apparatus for fs-TPLIF of CO measurements in sooting flames (L_1 *and* L_2 lenses, *BD* beam dump)

The experimental apparatus, shown in Fig. 2, consists of a regeneratively amplified Ti:sapphire laser system (Spectra Physics, Model: Solstice Ace) generating approximately 80-fs-duration laser pulses at 1-kHz repetition rate which pumps an optical parametric amplifier (OPA). The output energy of the pump laser at 800 nm was approximately 6 mJ/pulse. The signal beam generated from the parametric conversion process was subsequently frequency-doubled twice, and mixed with a portion of the fresh 800-nm beam to generate UV radiation near 230.1 nm with approximate energy of 40 μJ/pulse. The spectral bandwidth of the UV laser was approximately 0.8 nm full-width half maximum (FWHM), measured using a fiber-coupled spectrometer (Ocean Optics, Model Flame S). This UV laser beam was then guided to the probe region using several 45° dielectric laser mirrors and focused onto the probe region using a + 200-mm-focal-length plano-convex lens (LEO, UF-PX-25.4-200-200-230). A thin, variable ND filter (Thorlabs, NDC-100C-4M) was placed before the plano-convex lens to adjust the laser pulse energy in the probe region.

For initial CO spectroscopic studies, a static gas cell having effective optical path of 20 cm and four orthogonal fused-silica windows was placed in the probe region where the burner is located. The gas cell was vacuumed down to 10^{-3} Torr or better, using a vacuum pump prior to filling in pure CO. The pressure was monitored using a pressure transducer (Omega, Model: PX409-150AUSBH). Subsequently, for CO measurements in flames, the gas cell was replaced by a 25.4-mm × 25.4-mm Hencken calibration burner. The Hencken burner was operated on methane–air and ethylene–air flames over a wide range of equivalence ratios from very lean to rich conditions, and the probe volume was set approximately 10 mm above the burner surface. The flow rates of gases were regulated by mass flow controllers (MKS Instruments, GE50 series).

The fluorescence signal was collected orthogonal to the beam path using an intensified CCD (ICCD) camera (Princeton Instruments, Model: PIMax4). Also, a collimator coupled with a fiber optic cable was placed orthogonal to the beam path to collect the CO-TPLIF signal, which was transmitted to the entrance slit of a spectrometer (Princeton Instruments Model: IsoPlane 160) using a fiber optic cable consisting of a circular-to-linear fiber array. The spectrometer had multiple high- and low-resolution gratings although a 300 lines/mm grating was used during the present study. The vertical entrance slit width was set at 150 μm and the ICCD camera was mounted on the exit plane to record the spectra. The detection gate width and gain of the ICCD camera were set to 100 ns and 10% for the spectroscopic studies, and 10 ns and 60% for the imaging measurements, respectively. The spectrometer/ICCD camera system was wavelength and intensity calibrated using a set of calibration lamps (Princeton Instruments Model: IntelliCal®). The calibration system consists of a dual Hg, and a Ne–Ar lamp as well as a calibrated LED-based light source for intensity calibration.

3 Results and discussion

The TPLIF spectra of CO following the 230.1-nm fs excitation scheme were first studied using pure CO filled in the gas cell at a pressure of 1 bar. The resultant fluorescence emission spectrum is shown in Fig. 3. The fluorescence emission bands were detected at approximately 451, 483, 519, 561 and 608 nm in the Ångström band ($B^1\Sigma^+ \rightarrow A^1\prod$). Furthermore, because of the close energy level between the $b^3\Sigma^+$ triplet state and the $B^1\Sigma^+$ singlet state [31], the fluorescence emission could be also seen in the region of 282–380 nm originating from the third positive band ($b^3\Sigma^+ \rightarrow a^3\prod$)

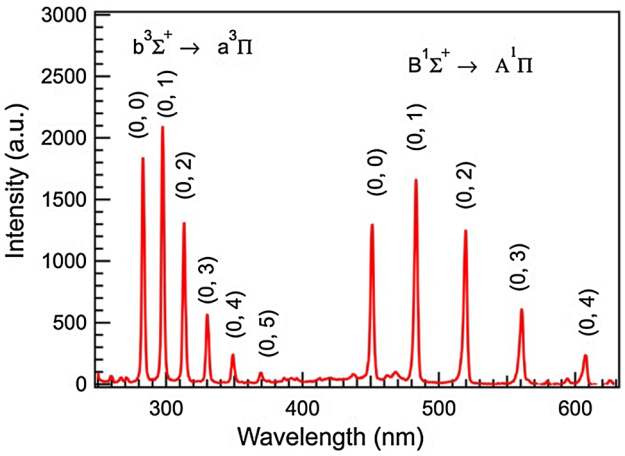

Fig. 3 Experimentally recorded fs-TPLIF emission spectra of CO using pure CO in the gas cell at 1-bar pressure

populated through collisions. Both bands were verified to originate from CO radicals by tuning the laser wavelength substantially away from the CO resonance peak.

In combustion environments, a major complication for quantitative CO measurements in sooting flames is the interference from CH and C_2 emissions. Shown in Fig. 4 are the fluorescence spectra recorded in a C_2H_4–air sooting flame with equivalence ratio, $\Phi = 1.5$ for three different intensifier gate widths of 10, 100, and 1000 ns. The excitation laser energy used was 40 μJ/pulse. The isolated CH emission band near 430 nm, as well as the C_2 emission peaks at approximately 437 and 468, 515 nm partially overlap with the CO spectral lines. These laser-generated C_2 emissions were also confirmed by observing the emission spectrum at 10-ns detection gate while detuning the excitation laser away from the resonance peak. Hence, we conclude laser-generated C_2 interferences have a pronounced effect on CO fluorescence signal in fuel-rich flames. The C_2 production could be originated from photolysis of CO or soot, or three-photon dissociation processes in the vinyl radical (C_2H_3) and acetylene (C_2H_2) under fuel-rich conditions [20, 32]. Furthermore, the C_2 signal contribution becomes severe with increasing detection gate width. More importantly, with increasing detection gate width, the overlapped regions between the isolated CO peaks around 451 and 483 nm and C_2 spectral lines are widened at the base. This effect can be seen in Fig. 4c as compared to Fig. 4a, b, indicating that C_2 interferences became predominant at wider detection gates. From the spectral data shown in Fig. 4a–c, it was concluded that while a shorter, 10-ns detection gate width can effectively eliminate nascent flame C_2 emissions, laser-generated C_2 interferences can still be present under these conditions.

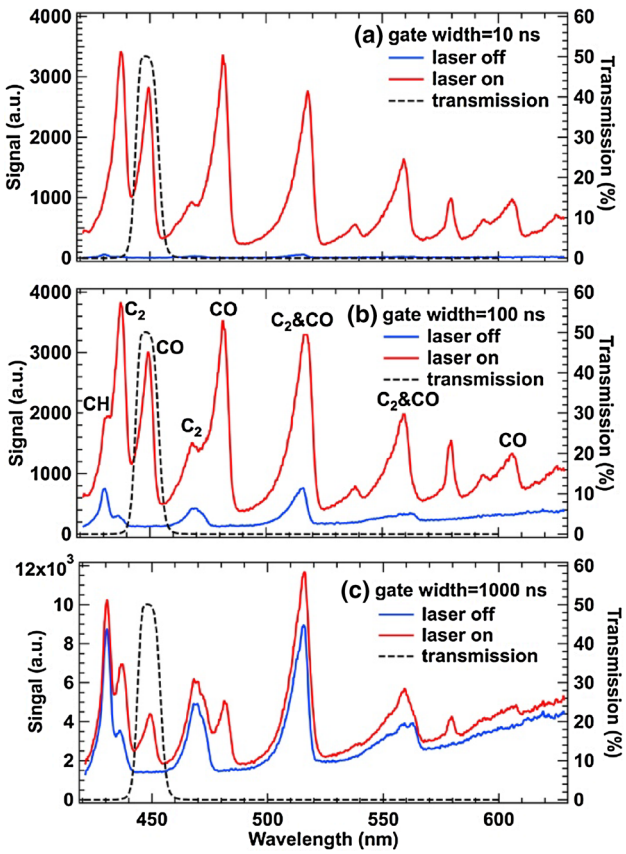

Fig. 4 C_2 interference for CO fluorescence in a C_2H_4–air sooting flame with equivalence ratio $\Phi = 1.5$. Detection gate width of **a** 10 ns, **b** 100 ns, and **c** 1000 ns. The transmission curve of the narrow-band spectral filter used for CO imaging is also shown by the dotted curve

Therefore, we incorporated a narrow-band pass filter (Thorlabs, FB450-10) to select only CO (0,0) Ångström emission band for CO-TPLIF measurements in sooting flames. The transmission curve of this filter is also shown by the dotted lines in Fig. 4. The detection gate width was maintained at 10 ns. Although this spectral filtering method also blocks portion of the CO fluorescence signal, we conclude that is an important measure to ensure the quantitative TPLIF detection of CO in heavily sooting flames. The C_2 spectral interferences were also investigated more carefully using a 3600 grooves/mm grating present in the same spectrometer. Although improved C_2 emission filtering may be possible by incorporating a custom-designed bandpass filter, such implementation is not justifiable because of the substantial additional cost and the possibility of variation in the spectral bandwidth due to minor angular changes when mounting the filter.

While a direct comparison of laser-generated C_2 emissions on the laser pulse width was not performed during the present study, the work by Brackman et al. [19] shows approximately a factor of 2 increase in C_2 emissions with respect to the CO peaks, when the laser excitation was changed from 10-ns pulses to 80-ps pulses. Furthermore, earlier work of H-atom [25, 26] and O-atom [27] TPLIF detection using fs pulses suggests a significant reduction in photolytic interferences as compared to ns and ps excitation schemes [33, 34]. Therefore, we expect a substantial reduction of laser-generated C_2 interferences on CO TPLIF detection when using low-average-power fs-duration pulses in the present study. A comprehensive investigation of photolytic effects is beyond the scope of the current work and will be the subject of a future study.

For the CO two-photon excitation, the resultant fluorescence signal is expected to be proportional to the square of the laser energy below the saturation regime. However, being a nonlinear loss mechanism of the excited state population, photoionization and stimulated emission can both result in sub-quadratic energy dependence of the fluorescence signal. The observed fs-TPLIF signal of CO in a $\Phi = 1.5$ sooting C_2H_4–air flame is plotted as a function of the laser pulse energy in Fig. 5. Because the spectral band of CO at 451 nm

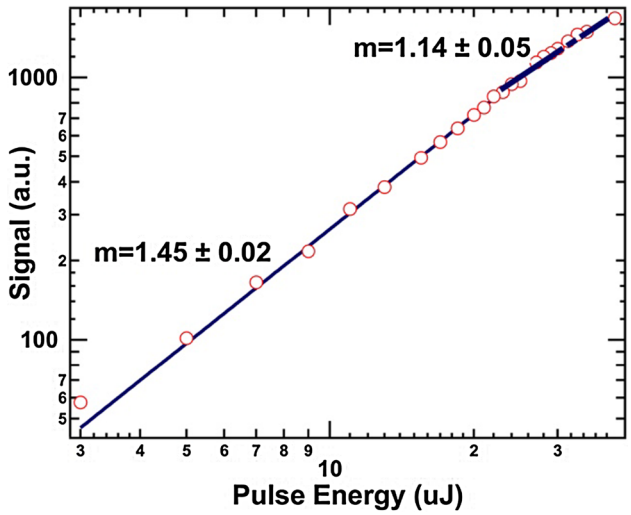

Fig. 5 Laser pulse energy dependence of fs-TPLIF of CO signal in a C_2H_4–air sooting flame with $\Phi = 1.5$

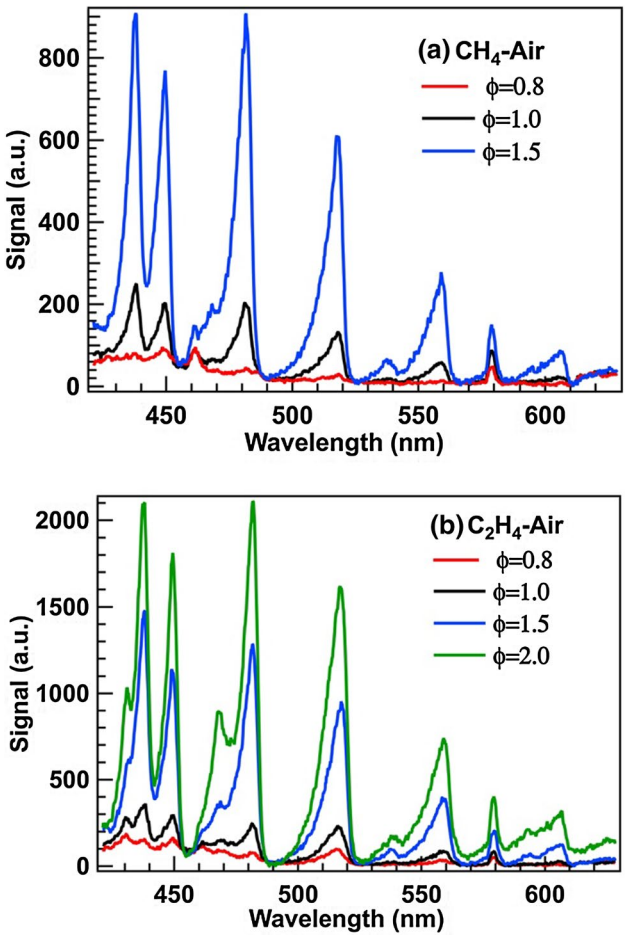

Fig. 6 CO-TPLIF emission spectra recorded at various equivalence ratios recorded in near-adiabatic premixed **a** CH_4/air, and **b** C_2H_4/air flames stabilized over the Hencken calibration burner

is nearly isolated from C_2 interferences, we only collected the CO fluorescence signal in the 450 ± 5 nm spectral range. The fluorescence signal plotted here is an average of 200 camera frames with each frame containing on-chip accumulation of 100 laser shots. Each data point was repeated three times and the average value is plotted. From these results, it can be seen that the fluorescence signal exhibits a power dependence P^m where the exponent $m = 1.45$ at lower laser energies, and $m = 1.14$ at higher laser energies. These results are in general agreement with previously reported values in the literature [1, 19, 35]. At low CO concentrations, higher laser energies are required to generate fluorescence signals with reasonable signal-to-noise ratio. However, at high laser energies, the ionization and stimulated emission processes become significant and can further reduce the expected quadratic power dependence for this two-photon excitation scheme [35].

After the characterization described in the above experiments, the fs-TPLIF scheme was then used to measure CO concentrations in a wide range of CH_4/air and C_2H_4/air sooting flames. These flames were stabilized over the Hencken calibration burner. For all these measurements, a 10-ns ICCD gate width was used along with the bandpass filter described above. The near-adiabatic flame conditions achievable in the Hencken burner allow direct comparison of the measured CO number density profiles with the calculated equilibrium CO number densities. The laser beam was passed approximately 10 mm above the burner surface and the laser pulse energy in the probe region was set at approximately 22 μJ/pulse. Figure 6 shows the CO-TPLIF emission spectra at various equivalence ratios in CH_4/air and C_2H_4/air sooting and non-sooting flames. It can be seen clearly that C_2 interferences become prominent with increasing equivalence ratio; even the isolated CO peaks around 451 and 483 nm are affected to some degree by neighboring strong C_2 emission bands despite time gating the signal using a 10-ns ICCD gate. Spectrally integrating the fluorescence signal only in the 445–455 nm region is the best possible solution to minimize C_2 interferences based on our current studies. The corresponding fs-TPLIF signal of CO as a function of flame equivalence ratio in CH_4/air and C_2H_4/air sooting flames is shown in Fig. 7. As discussed above, we used a 10-ns detection gate and only collected the CO fluorescence signal near 451-nm region using the bandpass filter to minimize the contributions from C_2 interferences. The equilibrium CO number densities were calculated using the STANJAN chemical equilibrium code and compared with the experimental CO fs-TPLIF profiles. It can be seen that the measured CO fluorescence signals agree with the calculated CO concentrations for both CH_4/air and C_2H_4/air flames over a wide range of equivalence ratios. The experimentally observed CO concentrations are lower than the equilibrium calculations at higher equivalence ratios or

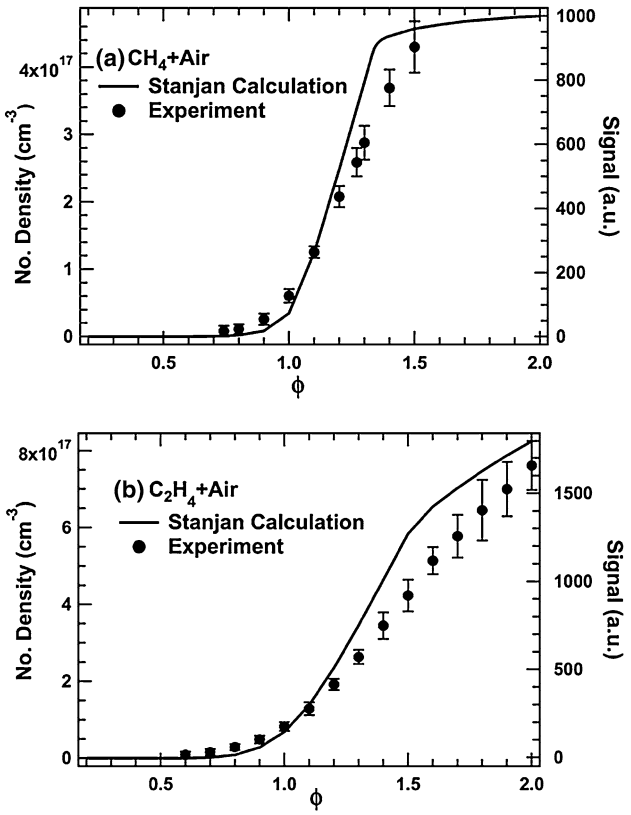

Fig. 7 Fs-TPLIF signal of CO as a function of flame equivalence ratio in **a** CH_4/air and **b** C_2H_4/air sooting flames. Solid lines represent the calculated equilibrium CO number density using STANJAN

fuel-rich conditions. Note that no quenching or photolytic interference (photodissociation of CO_2 and CO) corrections were applied for measured signals in these results. These observations suggest that the fs-TPLIF excitation scheme can provide significant advantages in quantitative detection of CO in sooting flames. A signal correction may be applied using respective quenching cross sections [7, 11], provided the flame temperature and major collision partner concentrations are known.

To illustrate the planar TPLIF imaging of CO in premixed sooting flames, the Hencken calibration burner was replaced with a premixed Bunsen-type jet flame. A + 100-mm-focal-length plano-convex lens coupled with a $f = -150$ mm plano-concave cylindrical lens was used to generate a laser sheet with an effective height of approximately 5 mm. A 50-mm-focal-length *f*/1.2 camera lens along with a 36-mm lens extension tube was used to collect the fluorescence signal and focus it onto the ICCD camera. The bandpass filter described above was mounted at the back end of the camera lens inside the lens extension tube. All images were acquired with a 10-ns detection gate width. The total laser energy used for the imaging measurements was ~ 25 μJ/pulse at the probe region. Sample fs-TPLIF images of CO in stable $C_2H_4/O_2/N_2$ jet flames at $\Phi = 1.0$, 1.5 and 2.0 are shown in Fig. 8. These images were generated by stacking a total of 60 images, each image containing on-chip accumulation of 200 laser shots. The burner was scanned vertically in steps of 0.5 mm between each image frame. As seen from these images, the CO-LIF signal exhibits a steep gradient in the transition between the cold reactants zone in the middle through the conical flame front, and gradually decays when moved radially outwards into the product zone and decays to near zero when entrained with the surrounding air. This behavior can be observed more clearly in Fig. 9, where the radial CO line profiles generated 10 mm above the nozzle exit are plotted. The corresponding vertical location is also indicated by the white lines in the CO images in Fig. 8. As seen in Fig. 9, the peak CO-TPLIF signals increase with increasing equivalence ratio.

The potential for the high repetition rate (i.e., 1 kHz), single-laser-shot CO detection was investigated by replacing the ICCD camera by a high-speed CMOS camera (Photron, Model: SA-Z) coupled with a high-speed intensifier (LaVision, Model: HS-IRO). Single-shot line images could be recorded using a 10-ns intensifier gate while incorporating the same spectral filter as described above. Statistics obtained from 1000 consecutive single-shot images recorded at 1-kHz repetition rate in a $\Phi = 1.2$ premixed $C_2H_4/O_2/N_2$ jet flame shows approximately 10% signal fluctuation, which is the percentage standard deviation of the mean. We believe these fluctuations to result from a combination of minor flame instability, shot-to-shot laser fluctuations and detection noise. It is important to consider such fluctuations when investigating spatially and temporally resolved CO measurements in turbulent sooting flames. The primary constraint for single-laser-shot 2D imaging in the current experimental setup is the limited laser energy available near 230 nm, thereby reducing the height of an excitation laser sheet only to a few millimeters. Also, the spectral filtering scheme implemented here limits the amount of CO fluorescence detected. However, such tight spectral filtering is essential for quantitative CO measurements in sooting flames as evident from the results of the present study.

4 Conclusions

We have demonstrated reduced-interference detection of CO in sooting hydrocarbon flames using fs-TPLIF. The broadband, two-photon excitation near 230.1 nm is followed by fluorescence emission collection in the Ångström band. However, the entire Ångström band emission in the 400–600 nm range cannot be utilized in fuel-rich sooting flames because of the C_2 Swan-band emissions from the flame as well as laser-generated photolytic interferences. Although laser-generated C_2 emissions can be reduced using

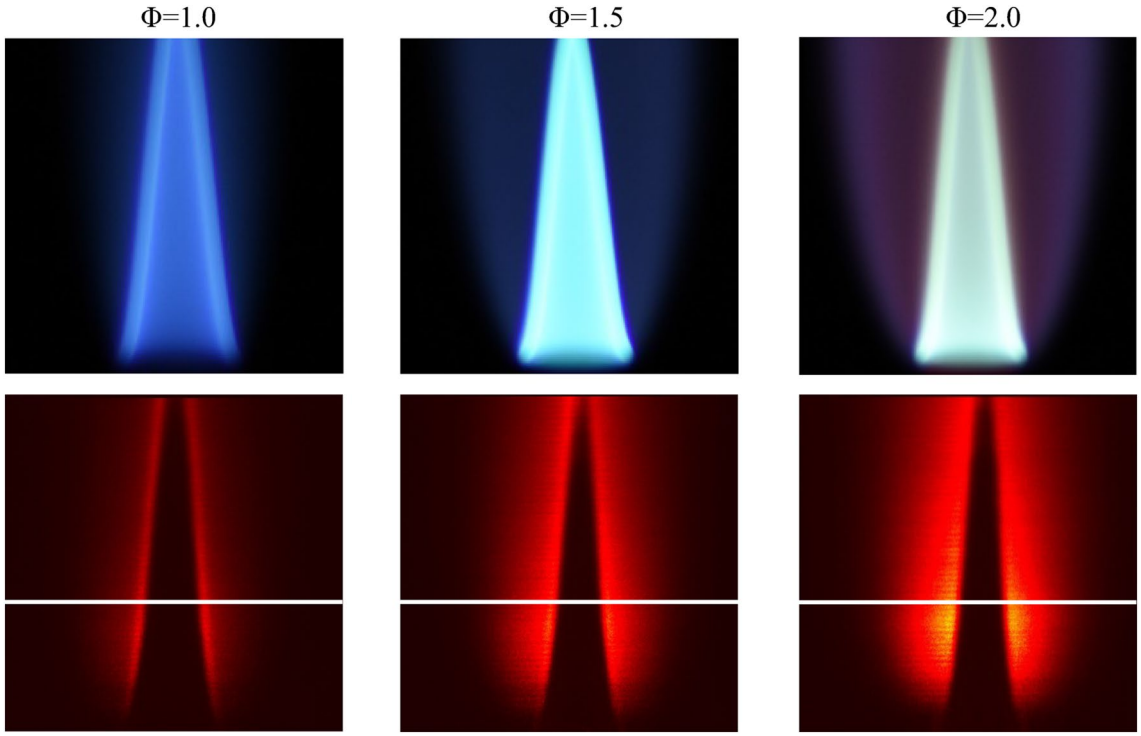

Fig. 8 Fs-TPLIF images of CO recorded at three different equivalence ratios in $C_2H_4/O_2/N_2$ jet flames. The top row shows digital photographs of the three flames, whereas the bottom row shows corresponding CO TPLIF profiles assembles as described in the text. Each frame corresponds to an area of 20 mm × 20 mm

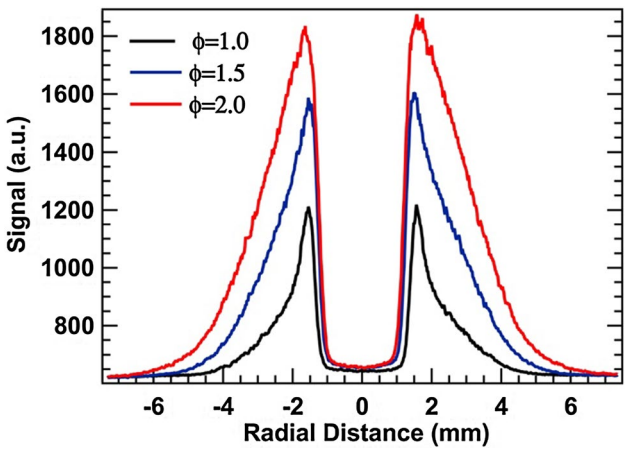

Fig. 9 Fs-TPLIF line profiles of CO at varying equivalence ratios in $C_2H_4/O_2/N_2$ jet sooting flames at 10 mm above the nozzle exit, the location shown by the horizontal white lines in Fig. 8

low-average-power fs pulses, complete elimination of such interference becomes rather difficult. The present study suggests carefully selected spectral filtering coupled with signal time gating in the order of 10 ns is required for reduced-interference CO detection in sooting hydrocarbon flames. The observed less than quadratic laser energy dependence of the CO fluorescence signal is indicative of non-negligible photoionization and stimulated emission processes. Nevertheless, comparison of the measured CO fs-TPLIF signals with the calculated equilibrium CO number densities show good agreements for both CH_4/air and C_2H_4/air sooting flames in a wide range of equivalence ratios. Two-dimensional CO-TPLIF imaging in a range of premixed sooting flames as well as single-laser-shot line imaging at 1-kHz repetition rate are demonstrated.

Acknowledgements Funding support from the National Science Foundation (NSF), Combustion, Fire and Plasma Systems program (Award no. CBET-1604633).

References

1. A.P. Nefedov, V.A. Sinel'shchikov, A.D. Usachev, A.V. Zobnin, Photochemical effect in two-photon laser-induced fluorescence detection of carbon monoxide in hydrocarbon flames. Appl. Opt. **37**, 7729–7736 (1998)
2. K. Kohse-Hoinghaus, J.B. Jeffries, Applied Combustion Diagnostics. (Taylor and Francis, New York, 2002)
3. J. Rosell, J. Sjoholm, M. Richter, M. Alden, Comparison of three schemes of two-photon laser-induced fluorescence for CO detection in flames. Appl. Spectrosc. **67**, 314–320 (2013)

4. S. Linow, A. Dreizler, J. Janicka, E.P. Hassel, Comparison of two-photon excitation schemes for CO detection in flames. Appl. Phys. B **71**, 689–696 (2000)
5. D.R. Richardson, N.B. Jiang, D.L. Blunck, J.R. Gord, S. Roy, Characterization of inverse diffusion flames in vitiated cross flows via two-photon planar laser-induced fluorescence of CO and 2-D thermometry. Combust. Flame **168**, 270–285 (2016)
6. Y.-C. Chien, D. Escofet-Martin, D. Dunn-Rankin, CO emission from an impinging non-premixed flame. Combust. Flame **174**, 16–24 (2016)
7. A. Singh, M. Mann, T. Kissel, J. Brubach, A. Dreizler, Simultaneous measurements of temperature and CO concentration in stagnation stabilized flames. Flow Turbul. Combust. **90**, 723–739 (2013)
8. J.H. Frank, S.A. Kaiser, M.B. Long, Reaction-rate, mixture-fraction, and temperature imaging in turbulent methane/air jet flames. Proc. Combust. Inst. **29**, 2687–2694 (2002)
9. N. Georgiev, M. Alden, Two-dimensional imaging of flame species using two-photon laser-induced fluorescence. Appl. Spectrosc. **51**, 1229–1237 (1997)
10. M. Alden, S. Wallin, W. Wendt, Applications of 2-photon absorption for detection of CO in combustion gases. Appl. Phys. B **33**, 205–212 (1984)
11. T.B. Settersten, A. Dreizler, R.L. Farrow, Temperature- and species-dependent quenching of COB probed by two-photon laser-induced fluorescence using a picosecond laser. J. Chem. Phys. **117**, 3173–3179 (2002)
12. F. Di Teodoro, J.E. Rehm, R.L. Farrow, P.H. Paul, Collisional quenching of CO $B^1\Sigma^+$ ($v' = 0$) probed by two-photon laser-induced fluorescence using a picosecond laser. J. Chem. Phys. **113**, 3046–3054 (2000)
13. M.D. Di Rosa, R.L. Farrow, Cross sections of photoionization and ac Stark shift measured from Doppler-free B ← X(0,0) excitation spectra of CO. J. Opt. Soc. Am. B **16**, 861–870 (1999)
14. M.D. Di Rosa, R.L. Farrow, Two-photon excitation cross section of the B ← X(0,0) band of CO measured by direct absorption. J. Opt. Soc. Am. B Opt. Phys. **16**, 1988–1994 (1999)
15. N. Georgiev, K. Nyholm, R. Fritzon, M. Alden, Developments of the amplified stimulated stimulated-emission technique for spatially-resolved species detection in flames. Opt. Commun. **108**, 71–76 (1994)
16. S. Agrup, M. Aldén, Measurements of the collisionally quenched lifetime of CO in hydrocarbon flames. Appl. Spectrosc. **48**, 1118–1124 (1994)
17. M.D.D. Rosa, R.L. Farrow, Temperature-dependent collisional broadening and shift of Q-branch transitions in the B ← X(0,0) band of CO perturbed by N_2, CO_2 and CO. J. Quant. Spectrosc. Radiat. Transf. **68**, 363–375 (2001)
18. J.E.M. Goldsmith, D.T.B. Kearsley, C2 creation, emission, and laser-induced fluorescence in flames and cold gases. Appl. Phys. B **50**, 371–379 (1990)
19. C. Brackmann, J. Sjoholm, J. Rosell, M. Richter, J. Bood, M. Alden, Picosecond excitation for reduction of photolytic effects in two-photon laser-induced fluorescence of CO. Proc. Combust. Inst. **34**, 3541–3548 (2013)
20. D.L. Osborn, J.H. Frank, Laser-induced fragmentation fluorescence detection of the vinyl radical and acetylene. Chem. Phys. Lett. **349**, 43–50 (2001)
21. K. Seki, H. Okabe, Photodissociation of methylacetylene at 193 nm. J. Phys. Chem. **96**, 3345–3349 (1992)
22. B. Balko, J. Zhang, Y.-T. Lee, 193 nm photodissociation of acetylene. J. Chem. Phys. **94**, 7958–7966 (1991)
23. S.S. Dimov, C.R. Vidal, Cross section for electronic quenching of the CO $B^1\Sigma^+$ state in collisions with hydrogen and helium. Chem. Phys. Lett. **221**, 307–310 (1994)
24. G.W. Loge, J.J. Tiee, F.B. Wampler, Multiphoton induced fluorescence and ionization of carbon monoxide ($B^1\Sigma^+$). J. Chem. Phys. **79**, 196–202 (1983)
25. W.D. Kulatilaka, J.R. Gord, V.R. Katta, S. Roy, Photolytic-interference-free, femtosecond two-photon fluorescence imaging of atomic hydrogen. Opt. Lett. **37**, 3051–3053 (2012)
26. W.D. Kulatilaka, J.R. Gord, S. Roy, Femtosecond two-photon LIF imaging of atomic species using a frequency-quadrupled Ti:sapphire laser. Appl. Phys. B **116**, 7–13 (2014)
27. W.D. Kulatilaka, S. Roy, N. Jiang, J.R. Gord, Photolytic-interference-free, femtosecond, two-photon laser-induced fluorescence imaging of atomic oxygen in flames. Appl. Phys. B **122**, 1–7 (2016)
28. J.B. Schmidt, B.L. Sands, W.D. Kulatilaka, S. Roy, J. Scofield, J.R. Gord, Femtosecond, two-photon laser-induced fluorescence imaging of atomic oxygen in an atmospheric-pressure plasma jet. Plasma Sources Sci. Technol. **24**, 032004 (2015)
29. C.A. Hall, W.D. Kulatilaka, J.R. Gord, R.W. Pitz, Quantitative atomic hydrogen measurements in premixed hydrogen tubular flames. Combust. Flame **161**, 2924–2932 (2014)
30. D.R. Richardson, S. Roy, J.R. Gord, Femtosecond, two-photon, planar laser-induced fluorescence of carbon monoxide in flames. Opt. Lett. **42**, 875–878 (2017)
31. K.P. Huber, G. Herzberg, Molecular Spectra And Molecular Structure, IV. Constants of Diatomic Molecules. (Van Nostrand Reinhold, New York, 1979)
32. J.M. Seitzman, J. Haumann, R.K. Hanson, Quantitative 2-photon LIF imaging of carbon-monoxide in combustion gases. Appl. Opt. **26**, 2892–2899 (1987)
33. W.D. Kulatilaka, J.H. Frank, T.B. Settersten, Interference-free two-photon LIF imaging of atomic hydrogen in flames using picosecond excitation. Proc. Combust. Inst. **32**, 955–962 (2009)
34. W.D. Kulatilaka, J.H. Frank, B.D. Paterson, T.B. Settersten, Analysis of 205-nm photolytic production of atomic hydrogen in methane flames. Appl. Phys. B **97**, 227–242 (2009)
35. P.J.H. Tjossem, K.C. Smyth, Multiphoton excitation spectroscopy of the $B^1\Sigma^+$ and $C^1\Sigma^+$ Rydberg states of CO. J. Chem. Phys. **91**, 2041–2048 (1989)